Status of Halbach Magnets for Cbeta

Stephen Brooks, Nick Tsoupas, 2016-Feb-24

1. Motivation

The Cbeta project has requirements for an FFAG arc with radius no more than 5 metres that bends electron energies of up to 250MeV.

The maximum radius is dictated by the available space in the L0E hall at Cornell University, so as to leave space for shielding blocks and movement of people, while not penetrating outside the overall walls of the building or into areas used for other equipment. The building itself is authorised for radiation sources like accelerators, while the outside is not, so the hall footprint is a fairly hard limit that would require permits and extensive construction work to circumvent.

The energy of 250MeV is designed to fit in with the FFAG 4x momentum range, the Cornell cryomodule energy gain and potential physics applications of the circulating beam. The FFAG momentum range is designed to bracket recent eRHIC designs that used 3x and 4x ranges in their FFAGs and is a significant advancement over the 2x range of EMMA. Although initially the cryomodule was specified for "100MeV", this is an absolute maximum and running with an FFAG requires a specific energy that has a high degree of confidence of being achieved. The current design therefore calls for 61MeV energy gain per turn, which has been verified as possible in tests even with one cavity not running. With a 6MeV injector this makes for a maximum energy in the FFAG of 6MeV+4*61MeV=250MeV. The physics applications and requirements are available from references in section 2 of http://arxiv.org/pdf/1504.00588v1.pdf. They prefer a higher energy, up to 300MeV ideally, although 250MeV is an acceptable compromise. Reduction to 200MeV energy would make the magnets somewhat smaller and lower-field but would not change any of the main challenges in the Halbach design, which looks like it works at 250MeV.

Given these parameters, the FFAG lattice puts fairly challenging requirements on the magnets in the arc. FFAGs are machines which intrinsically require a high gradient in the magnets, so the varying field can transport the very wide range of energies. This leads to high gradient magnets with short focussing periods. In Cbeta, the small arc radius also shortens the magnets and increases the required dipole and quadrupole fields, both in dipole and quadrupole, although it should be noted in FFAGs the "quadrupole component" is often the main bending field since the electron bunches are circulating off-axis.

Forcing the focussing periods to be longer would increase the separation of the different energy beams roughly by the square of the focussing length, so the magnets would get wider faster than they get longer, actually making the aspect ratio unfavourable. Shortening the periods would lead to theoretically narrow, but extremely high-gradient magnets that would not be wide enough to accommodate the vacuum chamber. To take account of this, an additional design constraint was added that the distance from the physical magnet pole to the ideal centroid of any of the beam orbits must be at least 17mm. This consists partly of 12mm clearance between the beam centre and the inner wall of the vacuum chamber, to fit the beam size, possible halo, allow for steering errors

and reduce resistive wall effects from going too close to the wall. A further 5mm allows for the thickness of the vacuum chamber, which can be up to 3mm for extruded parts, some mechanical clearance, plus 1mm for shims to be placed inside the magnet bore if necessary.

In an initial round of studies, a magnet design that uses iron poles driven by permanent magnets was found to be difficult to satisfy the contraints of the FFAG design. So the Halbach design with bare blocks of magnet arranged around the aperture was investigated as an alternative, because Halbach dipoles are known for being able to achieve very high fields. This yielded designs compatible with the FFAG lattice, subject to a few details later in this report. It should be noted that while the dipole achievable in the Halbach magnet is theoretically unlimited (the magnet outer radius expands exponentially with field), the quadrupole pole-tip field is not. There is a hard limit of gradient*bore for any given material grade, which the FFAG lattice has to avoid. It should also be noted that more recent co-optimisation of the iron-dominated magnet design with the FFAG lattice is showing that the iron pole design may in fact be possible, avoiding some of the complications of the Halbach arrangement (this work is currently being conducted by Holger Witte and J. Scott Berg).

The most recent Cbeta FFAG arc lattice using the Halbach type magnets is called Cell_Smoothpipe_2016-02-04. The magnet requirements for this cell, which consists of one focussing (QF) and one defocussing and bending (BD) magnet, are shown in the table below.

Parameter	QF magnet	BD magnet
Length	96.3mm	126.4mm
Gradient	-28.80 T/m	19.19 T/m
Dipole component at centre	0	-0.2680 T
Max good field radius	19.5mm	19.5mm
Min inner radius	36.5mm	36.5mm
Max outer radius	70.2mm	69.3mm
Max field in good field region	0.56 T	0.64 T
Max field at “pole tip”	1.05 T	0.97 T

These parameters were derived from optimisation of the cell in the Muon1 tracking code, subject to the various constraints described above, plus additional optical stability conditions. The figure of merit for the optimisation was to reduce the largest outer magnet radius in the cell, since window-frame correctors are under consideration for being wrapped outside these magnets, meaning a small radius will reduce power requirements as well as being more economical on magnet material.

2. Comparison of Features vs. Iron Poled Magnets

A summary table is provided below to illustrate the technology differences between choosing a Halbach magnet design and an iron-dominated permanent magnet design in an accelerator. Permanent magnet materials all have a temperature dependence and this can be compensated in the magnet in various ways. The iron quadrupole uses a technique from the Fermilab recycler where the permanent magnet blocks sandwiched in the iron yoke are mixed with NiFe alloy whose magnetisation contribution varies in the opposite way as magnetisation of the blocks, to provide a temperature range of 20°C or more with virtually no field strength variation. In the Halbach magnets, the field and magnetisation directions are not parallel, so this method does not work because the NiFe alloy would not provide compensating magnetisation in the correct direction. Instead, the dipole and quadrupole correctors, which would be present in the design anyway, are used to compensate the field variation, which manifests as an overall reduction factor in field strength and is therefore linear as a function of position like the magnets themselves.

	Iron Poles	Halbach
Field quality + tuning	Determined by iron pole shape. Adjustment would be via conventional pole shimming.	Determined by block magnetisation vectors. Adjustment via floating shims/iron wires just inside aperture.
Field strength + tuning	Iron shunts to partially short-circuit flux applied to outside. Also block pre-measurement and sorting. EM quad corrector coils around poles.	Determined by block magnetisation vectors. Tune with EM normal quad and dipole online correctors (see 'correctors' below).
Temperature sensitivity + compensation	0.1%/K for NdFeB but can (at ~20% strength penalty) incorporate NiFe material to passively compensate.	0.1%/K for NdFeB, cancelled by using EM normal quad and dipole online correctors.
Cross-talk in doublet + compensation	Few percent cross-talk, can be corrected with shunts.	Negligible cross talk, mu~1 linear field superposition.
Correctors (online/EM)	Normal quadrupole can be coils would around each pole. Others require special coils put within the bore.	Window-frame outside Halbach magnet using field superposition, because Halbach is magnetically transparent.

To compensate temperature changes, the correctors could be set either using data from the orbit position feedback, or a local field monitor. If the corrector coils themselves are water-cooled (as they are in the most recent design), it is possible to circulate a layer of water just outside the Halbach magnet blocks first, to stabilise their temperature to the extent that temperature compensation of any sort is no longer needed.

3. Halbach Magnet Design

The optimised FFAG cell required the QF magnet to be very close to a symmetrical quadrupole, i.e. with zero field at the centre. To simplify matters, the bore location was adjusted slightly so that QF really was exactly symmetrical, so that its design is that of a conventional Halbach quadrupole. Cross-sections of the two magnets are shown in the figures below.

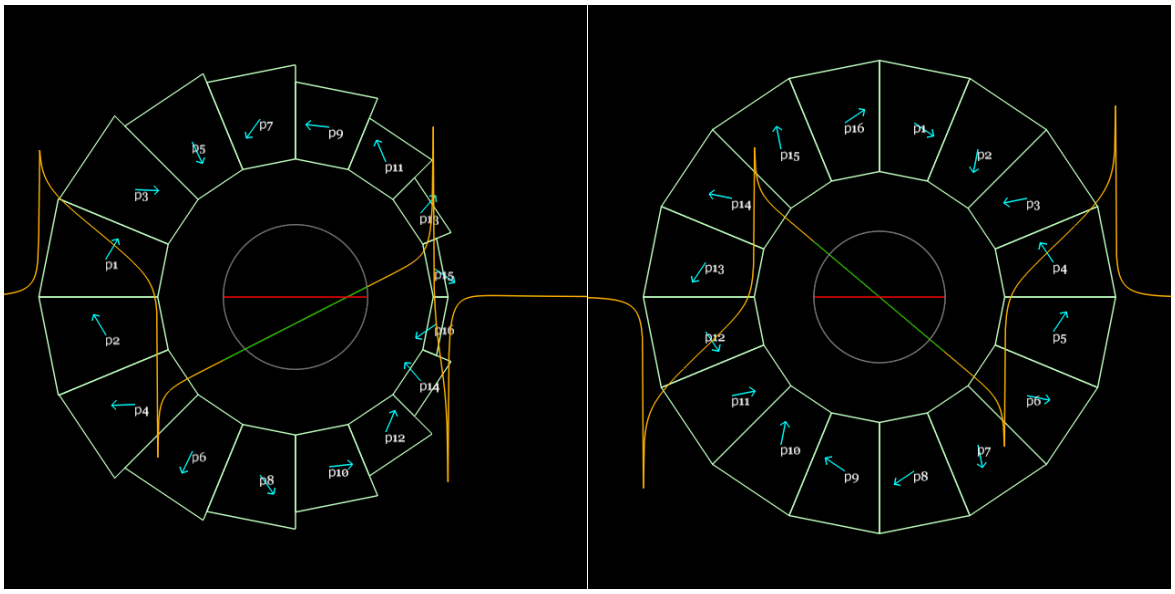

Figure. (Left) BD magnet. (Right) QF magnet. Orange graph is vertical field component B_y on the y=0 axis, with varying x position. The green segment is the field within the region required by the beams, which is supposed to be linear. Magnetisation axis is shown by blue arrows in each block.

The BD magnet on the other hand contains a significant dipole component: in fact, all the beams go through the negative B_y field region, which bends electrons clockwise in the L0E hall. The design of the BD magnet is also not a conventional Halbach arrangement: it requires a combination of dipole and quad, whereas conventional annular arrangements can only do one pure multipole at a time. It was considered to nest conventional dipole and quadrupole Halbach magnets but the outer magnet has to be quite large in that case. It was noticed that on one side of the nested magnet, the magnetisations were mostly cancelling anyway, so optimisation was run on a design with only a single layer of permanent magnet wedges, but with variable thickness and different magnetisation directions. This achieved a very accurate (<10^-5 in the linear model) combined function integrated field as required, a result that was replicated to high accuracy (~10^-4) by OPERA-3D simulations. It also uses much less material than a nested design.

3.1. Magnet Simulation and Codes

Two codes were used in the design and simulation of these Halbach magnets, which have shown good agreement as shown in this section. The simpler of the two is PM2D written by Stephen Brooks, which is a current sheet approximation of the fields from permanent magnet polygons in 2D. This provides an accurate model of the “average” field (integrated field divided by permanent magnet piece length) through the magnet, provided two conditions hold:

- The materials stay in the linear part of their B-H curve. In fact, if this is violated, the magnets will experience permanent demagnetisation, so any valid design ought to satisfy this

condition. PM2D can also evaluate the demagnetising flux from the other blocks at any point to ensure it does not go beyond the coercive force (H_cj) of the material.

- Mu_r=1 for all materials. This is almost true of NdFeB, which has a mu_r of about 1.025.

PM2D was used for the initial optimisation of the wedge sizes in the BD magnet, which tried to reduce the error multipoles to zero by changing their thickness and magnetisation direction independently keeping the required symmetry in the y=0 midplane. This requires many iterations of the design to be simulated, so a faster code is preferred during this design stage, before coordinates of the wedge corners are generated as input for the 3D magnet simulation.

The second code used, by Nick Tsoupas for 3D simulations, is OPERA-3D, which is industry standard. Very good agreement was attained between the two codes (on integrated field multipoles) when the materials were not in the demagnetising regime. Once the design was set, OPERA-3D was always used to do the final simulation and 3D field map generation.

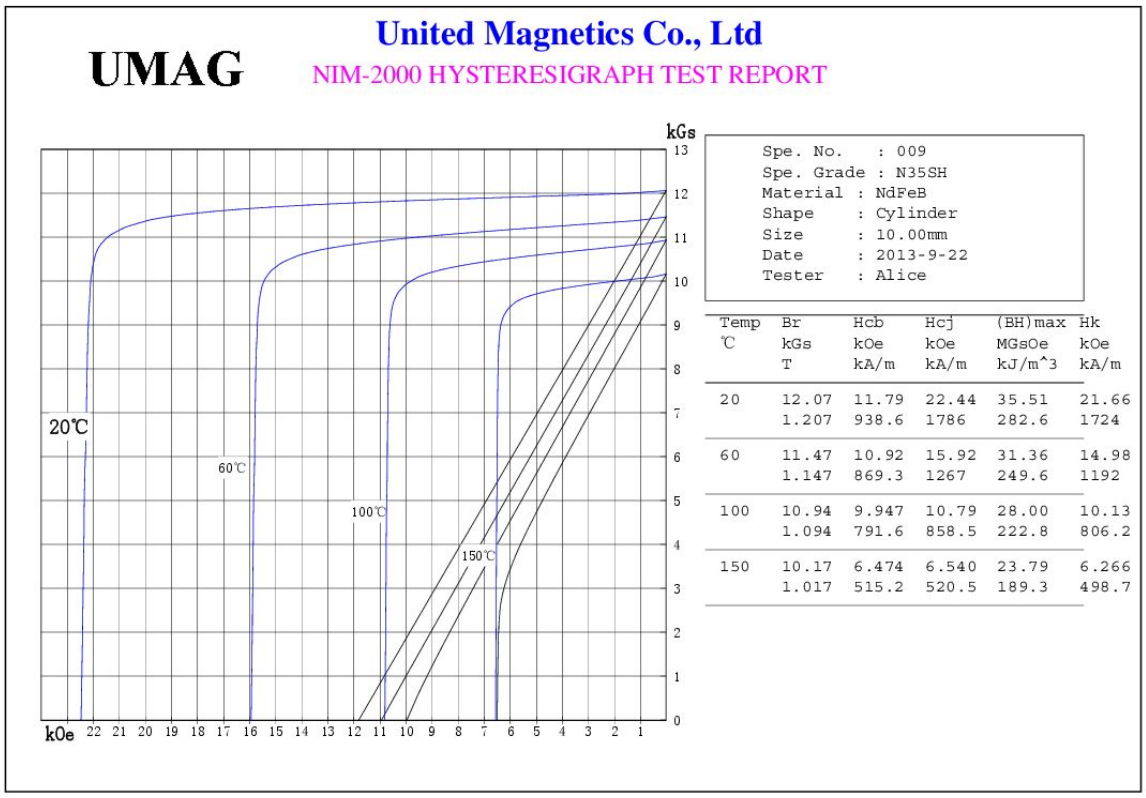

Figure. B-H curve of the AllStar Magnetics N35SH NdFeB permanent material, at various temperatures.

Running in OPERA-3D required that a specific material grade and B-H curve was chosen for the permanent magnet blocks. These grades and curves vary by manufacturer, so a grade from AllStar Magnetics was selected, which is the manufacturer for blocks for the Cbeta prototype magnets currently under order and shipping at the end of March 2016. The grade N35SH was selected, which combines a medium strength of 35 MGauss.Oe (the maximum available being ~52 MGauss.Oe) with a good resistance to external demagnetising fields. This is what the “SH” suffix means: a strong resistance to heat, which stems from its high H_cj demagnetising field value (2.24 T) at room temperature. The strength translates into a residual field B_r of 1.207 T.

After OPERA-3D models were run, a best fit with the magnetisation “B_r” value used in PM2D, which assumes mu_r=1, was found (1.1939 T), which represents the average magnetisation from the material including the small reduction from regions of reverse flux with mu_r being slightly larger than 1. This lies between B_r and H_cb of the material as expected. With this value, the PM2D designs could be loaded directly into OPERA-3D (with the N35SH material) and the strength would be correct, with no further design modifications required.

4. Tracking and Compatibility with FFAG Lattice

Once OPERA-3D field maps have been generated, they can be loaded back in to the Muon1 tracking code, which is the same code used for the original lattice optimisation done with field models rather than field maps.

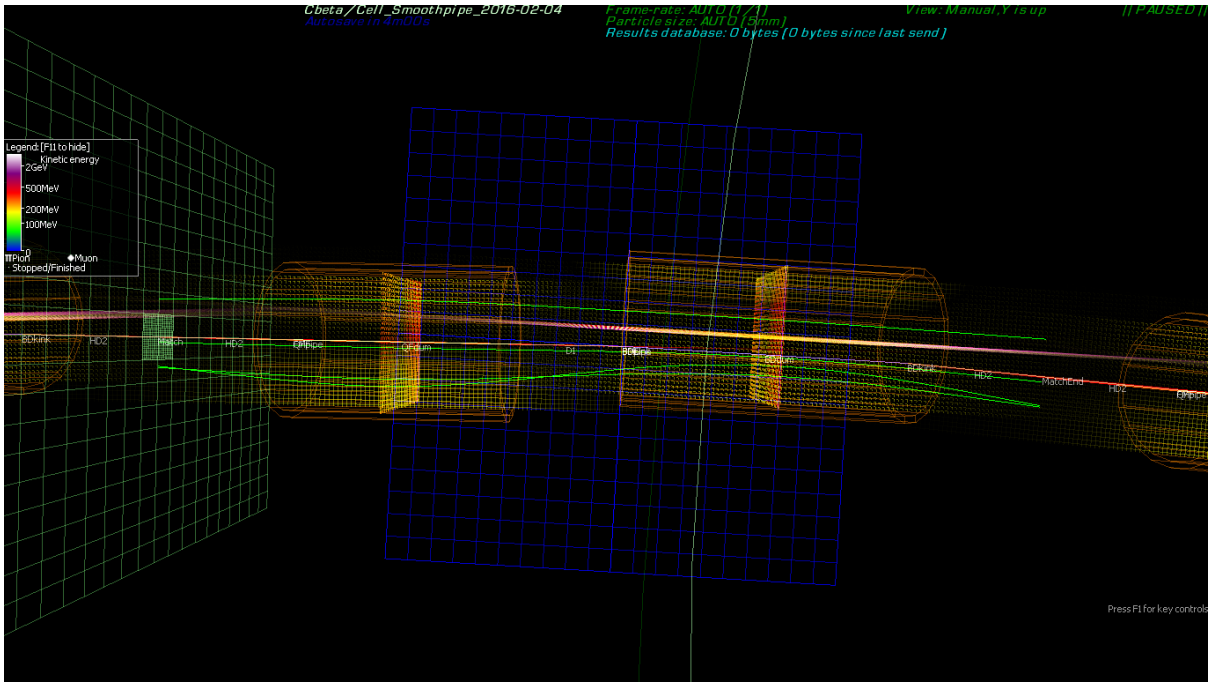

Figure. Matched orbits (green) for the four Cbeta energies through an FFAG arc cell made with OPERA-3D field maps generated from Halbach magnets. The orange cylinders represent the approximate apertures of the vacuum pipe and the grids are 1cm per square.

The figure above shows such a simulation, where Muon1 has found “closed orbits” for each energy, which exit the cell at the same position and angle that they enter. The closed orbits found through field maps will be slightly different than those found for the original field model in the lattice-design optimisation, but as shown in the graph and table below, the discrepancy is not very large (<1mm).

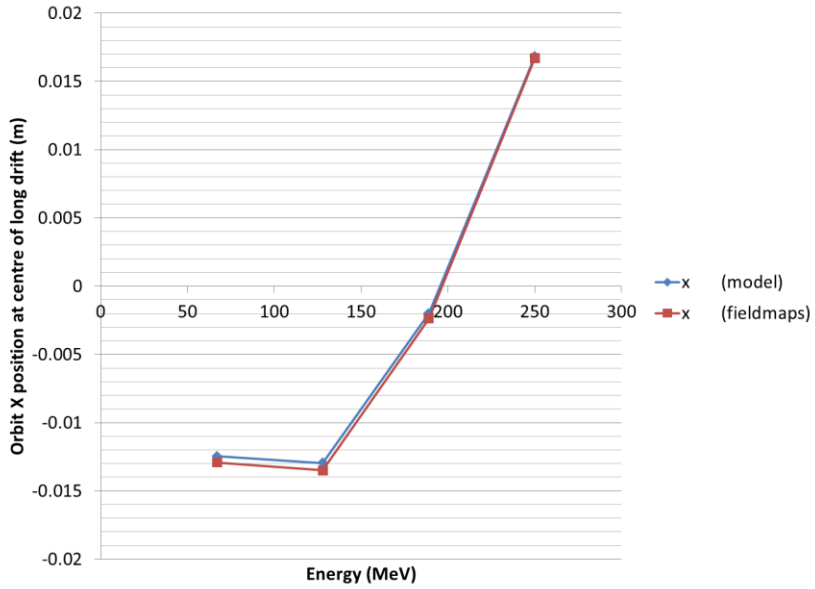

Energy (MeV)	x (m) (model)	x (m) (fieldmaps)
250	0.016825	0.01668
189	-0.00201	-0.00237
128	-0.01296	-0.01349
67	-0.01246	-0.01292

Figure & Table. Transverse position (X, in metres) of the four closed orbits, as a function of energy, at the midpoint of the long drift in the Cbeta FFAG arc cell. Blue dots are from a Muon1 simulation using field models and red dots from a Muon1 simulation using OPERA-3D field maps.

This good agreement is partly due to a fortunate choice of fringe field length in Muon1's soft-edged Maxwellian field model. Muon1 models the fall-off of multipole components near the entrance of exit of a magnet as proportional to ½ + ½ tanh(z/f) where z is the longitudinal position relative to the magnet end and f is a "fringe length" parameter (f). It was chosen to be 2.5cm here, roughly the same order of size as the magnet apertures. Detailed studies suggested the best agreement with these fieldmaps is obtained with f=2.7cm. For these short magnets in Cbeta, the fringe field makes up a large part of the field so it is important to include it consistently (some hard-edged models do not have good agreement with the optics).

The closed orbit matching process also determines the shape of the beam (optical alpha and beta functions) that will be preserved on traversing once through the cell. This also allows the single-cell tunes in the X and Y planes to be calculated. A similar comparison of tunes from the field map versus the original optimiser's field model is shown in the figure and table below.

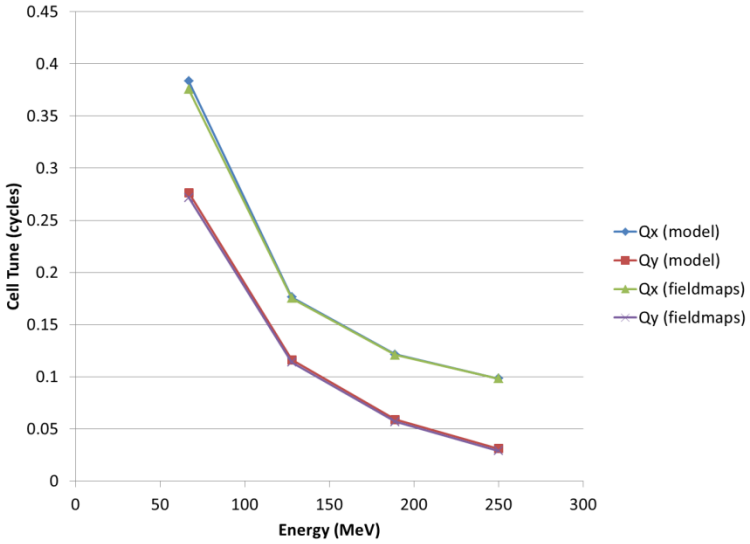

Energy (MeV)	Qx (model)	Qy (model)	Qx (fieldmaps)	Qy (fieldmaps)
250	0.098132	0.031006	0.098272	0.029062
189	0.121474	0.058797	0.120911	0.056874
128	0.176315	0.11615	0.175274	0.113949
67	0.383309	0.276579	0.375643	0.271753

Figure & Table. Comparison of the calculated X and Y tunes of the FFAG cell using Muon1's model field and OPERA-3D field maps.

The cell tunes are important because they determine the limits on the stability of the beam (0 and 0.5 being the unstable limits) and its response to errors, the tune determining the frequency of error oscillations. The largest discrepancy between field map and model field is found in the low-energy (67MeV) beam, where the model predicts 0.3833 and the field maps predict 0.3756, a difference of 0.0077 cycles per cell. This is not a large enough difference to put the beam into a resonance or drastically affect the optical behaviour of the machine.

5. Window-Frame Correctors

The property of the permanent magnets to be magnetically saturated allows superposition of the magnetic fields and therefore permanent magnets can accept electromagnets as corrector magnets with no distortion of the their magnetic field. Figure1 is an isometric view of an OPERA model of a Halbach-type magnet surrounded by a window frame electromagnet acting as a corrector.

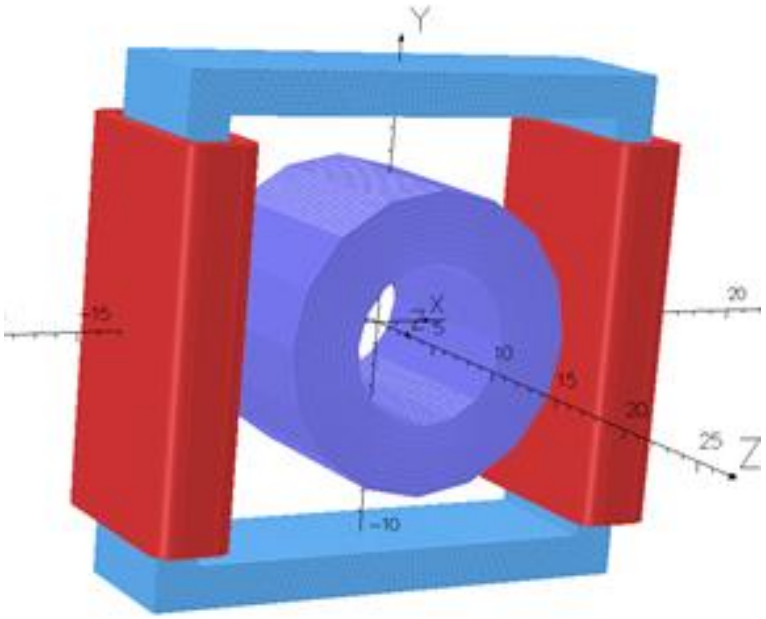

Figure 1. A window frame magnet with two coils generates a normal dipole field which is superimposed on the field of the permanent magnet.

In this section we will present results from the 3D OPERA calculations which prove the following statements:

1. The window frame magnets in spite their large aperture and short length, do not excite significant transverse magnetic multipoles except the ones are designed to produce.
2. An excited window frame magnet placed around a Halbach-type permanent magnet as in Fig. 1 does not alter significantly the multipoles of the Halbach-type magnet (measurements are under way) and there is an almost perfect superposition of the fields of the two magnets.
3. The Halbach-type magnets lend themselves easily to window-frame corrector magnets and do not interfere with possible access to the beam instrumentation which is placed in the short drift spaces between the magnets.
4. Four Halbach-type magnets were placed next to each other along their symmetry axis with the magnets touching each other and the integrated multipoles of all four magnets was measured to be equal to the sum of the of the integrated multipoles of each magnet measured separately. This measurement provides an almost perfect proof of field superposition. (Measurements have been made thus no results from calculations will be presented).

5.1. The B_field of a Window-Frame Electromagnet

Figure 2 is a picture of 3D OPERA model window frame magnet to be used as corrector around a Halbach-magnet.

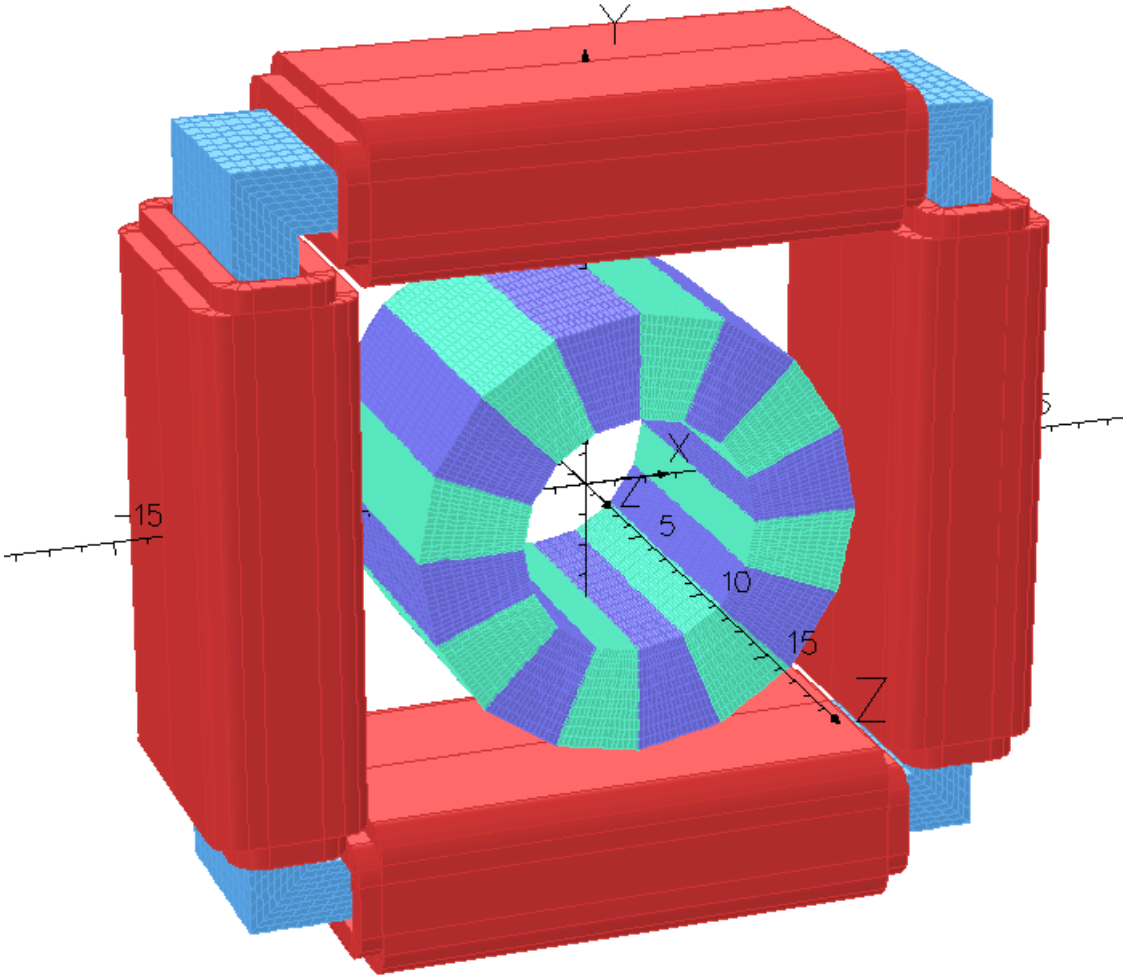

Figure 2. A window frame magnet with eight coils acting as normal and skew dipoles, and a normal quadrupole. By rotating the window frame by 45^{o} we can generate a skew quadrupole instead of normal one.

Figure 3 below is a projection on the x,y plane of the window frame magnet which shows that the maximum transverse directions of the corrector magnet surrounding a Halbach magnet is less than 30 cm.

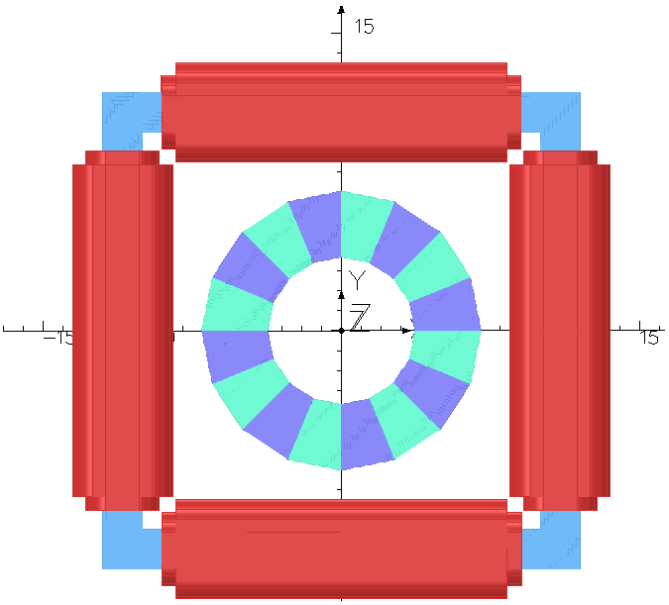

Figure 3. The projection of the window frame magnet on the x,y plane. The maximum transverse extend of the magnet is less than 30 cm.

Table I shows the integrated magnetic multipoles at R=1 cm of three different configurations of a quadrupole Halbach magnet and dipole window frame magnet. The 2nd row shows the integrated multipoles a dipole window frame magnet with no permanent magnet inside. Row 3 shows the integrated multipoles of a quadrupole Halbach-type magnet with no excitation of the dipole corrector and row 4 the multipoles of the dipoles window frame magnet excited, surrounding the quadrupole Halbach-type magnet. The permanent magnet material of the quadrupole magnet is NdFeB-N35 and the BH-curve for this material is shown in Fig. 4. The results from Table I show that the field of the window frame magnet is simply superimposed on the field of the quadrupole magnet.

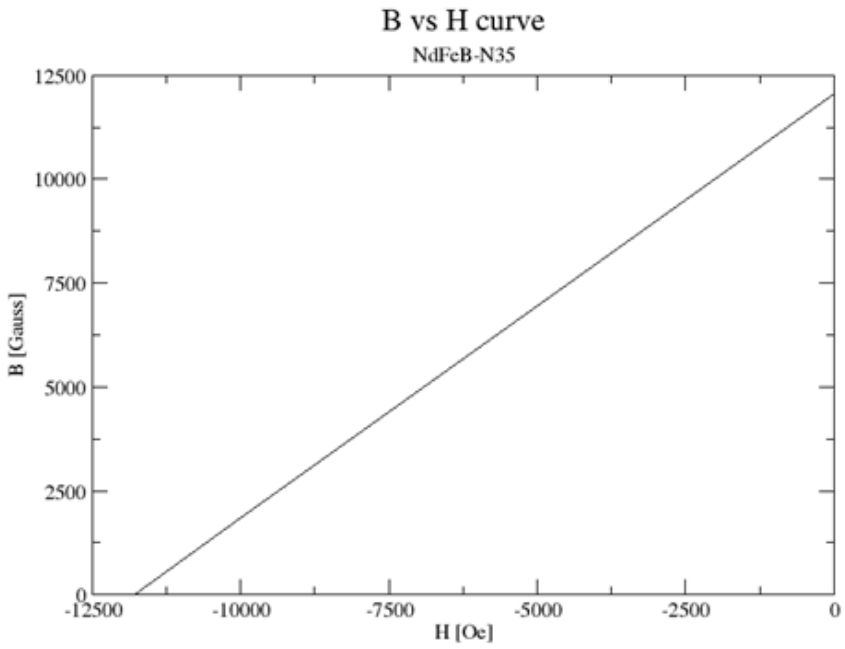

Figure 4. The BH curve of the NdFeB-N35 material.

Table I. The integrated magnetic multipoles of the window frame magnet by itself (2nd row) of a quadrupole Halbach type magnet (3rd row), and of the window frame magnet surrounding the quadrupole Halbach-type magnet.

	Dipole [Gauss.cm]	Quad [Gauss]	Sext. [Gauss.cm^{-1}]	Oct. [Gauss.cm^{-2}]	Dec. [Gauss.cm^{-3}]	12pole [Gauss.cm^{-4}]
WFonly	1931.14	-0.0013	1.02	0.00003	0.014	-0.000015
PM only	0.000003	27798.5	0.000003	0.00000002	0.000003	0.037
WF_PM	1933.7	27798.5	1.02	0.0123	0.017	0.016

The results of Table I corroborate the ideal superposition of the fields generated by a Halbach-type permanent magnet with the fields of the window-frame magnet. Experimental measurements to prove these results are under way.

Figure 5a is an isometric view of a few permanent magnets of the Cβ arc with correctors. This view shows that the window frame magnets do not extend into the drift space between the magnets. Figure 5b is the projection on the yz plane of the six magnets showing in Fig. 5a. The current through the coils of the window frame magnet can generate the required correction field for the permanent magnets.

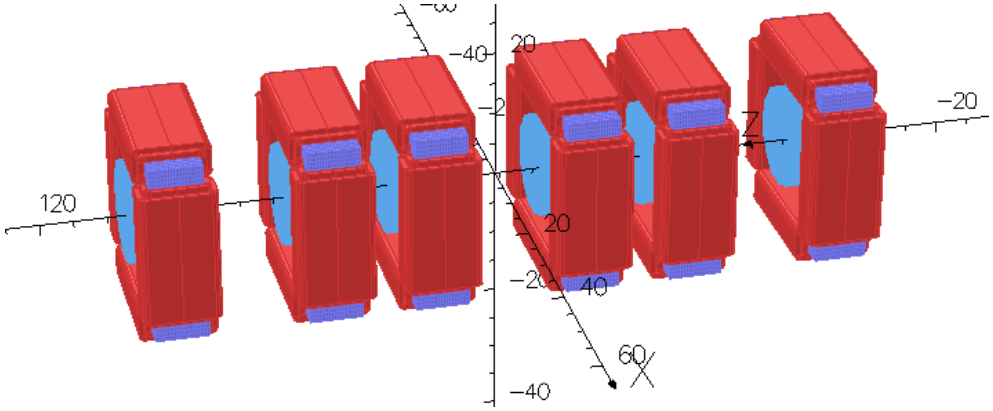

Figure 5a. Isometric view of six of the permanent magnets of the Cβ arc.

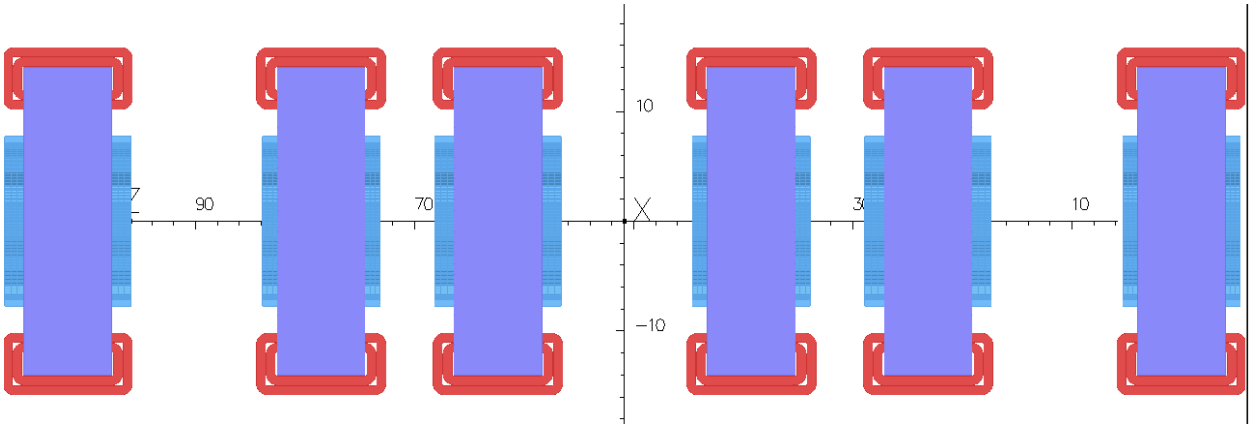

Figure 5b. Projection on yz plane of the six permanent magnets of the Cβ arc shown in Fig. 5a.

5.2. Power dissipation on the coils of the window frame magnets

The dipole corrector field of a window frame magnet is generated by two coils wound around two opposite sides of the window frame as shown in Figure 1. The required dipole corrector field is ±50 Gauss over the ~11 cm length of a permanent magnet. Calculations show that such a dipole field can be generated with two racetrack coils 8 mm thick as in Fig. 1, when a current density of 50 A/cm^2 flows through each of the racetrack coil.

The quadrupole corrector field is generated by four racetrack coils (Panofsky Quadrupole) wound each around each side of the window-frame, as shown in Fig. 2. The required quadrupole field is ±0.45 T/m over the ~11 cm length of a permanent magnet. Calculations show that such a quadrupole field can be generated with four racetrack coils 8 mm thick as in Fig. 2, when a current density of 375 A/cm^2 flows through each of the racetrack coil.

The coils of either dipole or quadrupole correctors will be made of a hollow copper conductor of an approximate cross-section of 6mmx6mm with a hole to carry cooling water to abduct the heat generated by the relative large current density of 375 A/cm^2 required to excite the quadrupole multipole. It it turns out that the power supply which will provide this large current density is expensive we may think of placing "additional copper" or increase the ampere turns of the quadrupole coils to reduce the current provided by the power supply.

The column 5 and 6 of Table II provides the power dissipation per unit length of each racetrack coil shown in figs 1,2,3,5, to generate dipole or quadrupole field. To find the actual power dissipated per corrector, the values of column 6 in Table I must be multiplied by the length of the racetrack coil.

Table I. Dissipated power in the racetrack coils to generate the required dipole or quadrupole field.

	Strength	# Racetrack coils	J [A/m^2]	Power/coil [W/m]	Power/corrector [W/m]
Dipole	±50 Gauss	2	50	6	12
Quadrupole	±0.45 T/m	4	375	150	600

5.3. Temperature Stabilisation

As water cooling will be used for the window-frame corrector coils, it is inexpensive to add an additional layer of water in the magnet holder to stabilise the temperature of the permanent magnet blocks. This ideally will be the first place the cool water flows, before it gets heated up in the hollow copper conductors. A schematic of this scheme is shown in the figure below.

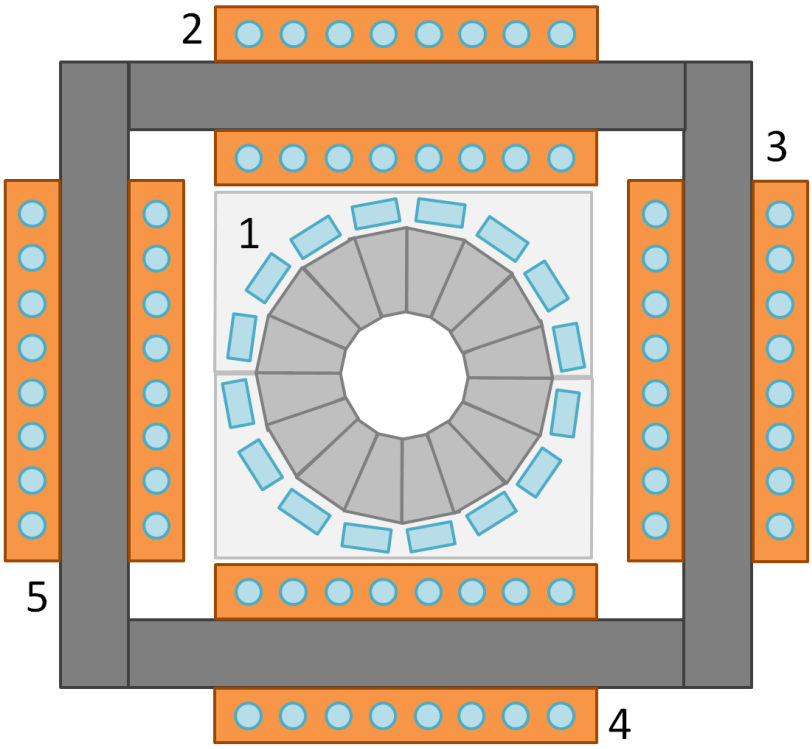

Figure. Schematic cross-section of the Halbach magnet and window-frame corrector assembly. Cooling water flows through channels in the magnet holder (1) before cooling the window frame corrector coils (2 through 5).

6. Halbach Magnet R&D and Shimming Results

BNL lab-directed R&D (LDRD) provided some money for constructing prototype permanent magnet quadrupoles for eRHIC, which is also an FFAG. Blocks were ordered from Shin-Etsu Corporation in August 2014 for three different designs, one of which was a Halbach quadrupole. The main differences between eRHIC and Cbeta magnets are that eRHIC requires an open midplane to allow synchrotron radiation to be dumped and eRHIC's magnets are ~1m long, an order of magnitude longer than Cbeta's. However, to reduce cost, the eRHIC prototype magnets were built in 6cm sections, roughly the longest piece of permanent magnet the company could magnetise at once.

The table below shows that the eRHIC prototype Halbach quadrupole is a good model for the Cbeta magnets too, at least until the parts for purpose-built Cbeta prototypes are delivered.

Table. Comparison of the Halbach shimming test magnet "5A" with requirements of Cbeta magnets.

Parameter	eRHIC prototype quad "5A"	Cβ requirement QF	Cβ requirement BD
Length	60.0mm	96.3mm	126.4mm
Gradient	27.5 T/m (measured)	-28.8 T/m	19.2 T/m
Central dipole	0 (by realignment)	0	-0.268 T
Material	SmCo R26HS (Shin-Etsu)	NdFeB N35SH (AllStar Magnetics)	NdFeB N35SH (AllStar Magnetics)
Min R of physical magnet pieces	22.5mm (design) 23.5mm (measured)	36.5mm	36.5mm
Max R of beam centroid	10mm (rotating coil) 15mm (extrapolated)	19.5mm	19.5mm
$\mathbf{R_{max,beam}/R_{min,magnet}}$	43% (coil) 64% (extrapolated)	53%	53%

The eRHIC magnet was constructed out of SmCo instead of NdFeB for historical reasons: concerns about radiation resistance, with SmCo being more resistant. Since then, a radiation test has shown NdFeB of an appropriate grade survives >100 Gy of radiation on the RHIC beam dump during a run. SmCo also contains much more cobalt, which can lead to long-term Co-60 activation.

6.1. Repeatability of Unshimmed Halbach Magnets

Five 6cm-long permanent magnet quadrupoles were made for eRHIC prototyping, of the kind shown in the figure below. Note that the holder was made on a 3D printer and the design for eRHIC incorporates mid-plane gaps for synchrotron radiation to exit.

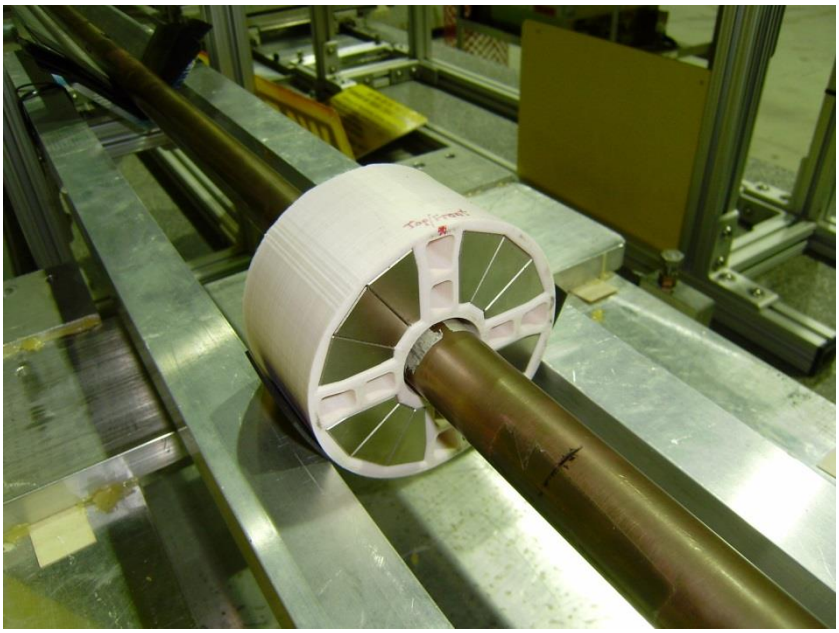

Figure. The 6cm-long eRHIC LDRD Halbach magnet being measured on the rotating coil at BNL's magnet division.

These were all measured on the BNL magnet division rotating coil to test the field quality of Halbach quadrupoles without shimming. Blocks from this factory, typically have 1-2% magnetisation strength error (the full width of magnetisation bins in the Shin-Etsu materials catalogue is ~5%) and ±1° magnetisation direction error, according to the supplier's quote. The five assemblies were measured on the rotating coil (not all the individual blocks), with results shown in the table below.

Table. Rotating coil measurements of 5 unshimmed Halbach permanent magnet quadrupoles.

Summary of field measurements in eRHIC Permanent Magnet Quadrupoles (27-Apr-2015)

Field harmonics are in "units" of 10^{-4} of the quadrupole field at a reference radius of 10 mm.

Quantity	PMQ_0001 Run 2	PMQ_0002 Run 3	PMQ_0003 Run 2	PMQ_0004 Run 3	PMQ_0005 Run 2
Integrated Gradient (T)	1.8647	1.9097	1.9053	1.8958	1.9024
Normal Dipole	--	--	--	--	--
Normal Quadrupole	10000.00	10000.00	10000.00	10000.00	10000.00
Normal Sextupole	27.83	-29.83	35.83	-4.53	-11.95
Normal Octupole	5.39	-3.12	32.81	16.50	3.61
Normal Decapole	-4.92	-2.44	2.90	7.09	3.86
Normal Dodecapole	-188.14	-194.57	-188.00	-192.96	-190.26
Normal 14-pole	-1.59	0.36	-0.67	0.43	1.03
Normal 16-pole	-0.44	-0.22	-1.10	-0.58	-1.31
Normal 18-pole	-0.24	0.19	-0.38	-0.25	0.07
Normal 20-pole	-2.37	-2.88	-3.13	-2.93	-2.91
Normal 22-pole	0.04	0.03	0.01	0.03	-0.01
Normal 24-pole	0.02	0.00	-0.02	0.01	0.04
Normal 26-pole	0.02	-0.01	0.02	-0.01	-0.02
Normal 28-pole	0.11	0.12	0.12	0.13	0.12
Normal 30-pole	0.00	0.00	0.00	0.00	0.00

Quantity	PMQ_0001 Run 2	PMQ_0002 Run 3	PMQ_0003 Run 2	PMQ_0004 Run 3	PMQ_0005 Run 2
Field Angle (mr)	--	--	--	--	--
Skew Dipole	--	--	--	--	--
Skew Quadrupole	--	--	--	--	--
Skew Sextupole	-16.41	1.90	-43.69	28.96	-5.28
Skew Octupole	-12.32	0.25	-12.55	4.03	-18.51
Skew Decapole	-11.98	-6.08	-5.68	-1.00	-8.52
Skew Dodecapole	-2.27	-0.99	-3.12	0.87	-4.96
Skew 14-pole	1.93	0.13	0.47	0.01	0.85
Skew 16-pole	-0.22	-0.09	-0.02	0.27	-0.13
Skew 18-pole	0.03	0.17	-0.06	0.05	0.10
Skew 20-pole	0.08	0.00	0.07	-0.20	0.01
Skew 22-pole	0.02	0.03	0.07	-0.05	0.00
Skew 24-pole	0.01	0.00	0.02	-0.02	0.01
Skew 26-pole	0.00	0.00	0.00	-0.01	0.01
Skew 28-pole	0.00	-0.01	0.00	0.01	0.00
Skew 30-pole	0.00	0.00	0.00	0.00	0.00

The Normal Dodecapole error of ~-190 units present in all magnets should be ignored for this comparison, since it was a systematic error made by the manufacturer using the wrong information for magnetising some of the blocks. This was compensated for in later designs by moving the blocks.

The raw magnets have sextupole error magnitudes (normal and skew added in quadrature) of 13-57 units; octupole errors of 3-35 units; decapole errors of 6-13 units, with poles above dodecapole being less than 3 units. A unit is 10^-4 relative to the main field, so these magnets are slightly better than 1% relative field error, which is roughly to be expected from the intrinsic magnetisation errors of the blocks they are made from. This on its own is not yet good enough for the 10^-3 level accuracy required by the accelerator, so shimming is required as described in the next section.

The coil is calibrated to measure at 1cm radius, which is smaller than the Cbeta orbit excursion but as shown in the previous table, the eRHIC prototype magnet had a smaller aperture overall.

6.2. Unshimmed Magnet Theoretical Error Study

Although the above experiment has shown what the field errors are in reality, it is also possible to put random magnetisation errors into the simulation code in order to find out how specifications on the magnetisation error range translate into average errors in the Halbach magnets.

Each block's magnetisation vector receives an independent random error. Since manufacturers give tolerances as total ranges (e.g. ±2.5% in strength), uniform distributions were used for these errors, with a parallel and perpendicular component being added for the magnetisation strength and angle errors respectively. In the study shown in the two tables below, two cases were considered: a fairly good case where the strength error is 1% and magnetisation direction is also accurate to 1% = 0.01 radians = 0.57 degrees; and the worst case where the strength error is the full range of a material grade of 2.5% and the angle error is the worst quoted spec from a manufacturer of 5 degrees.

Table. Average over many runs of the total error in units (10^-4 of the quadrupole amplitude), where the total error is the quadrature sum of all the normal and skew error poles, measured at the largest beam radius.

Magnet	Max magnetisation strength error	Max magnetiation direction error (radians)	Max magnetiation direction error (degrees)	Average total error (units = 10^-4 of quad)
QF	1.00%	0.01	0.572958	31
QF	2.50%	0.0873	5	212
BD	1.00%	0.01	0.572958	29
BD	2.50%	0.0873	5	201

Table. Multipole errors in two randomly-chosen instances of the QF magnet. (Left) a magnet with 1% magnetisation maximum amplitude error and 0.01rad maximum angle error. (Right) a magnet with 2.5% amplitude error and 5 degrees angle error.

Amplitudes in units: (norm=24.8715)

2-pole: -13.70	2-skew: 0.94
4-pole: 10000.00	4-skew: 5.05
6-pole: 13.10	6-skew: 14.75
8-pole: -1.21	8-skew: -2.76
10-pole: -0.58	10-skew: -0.20
12-pole: -0.70	12-skew: 1.49
14-pole: 1.66	14-skew: -0.28
16-pole: 0.20	16-skew: 0.07
18-pole: -0.03	18-skew: 0.01
20-pole: -0.04	20-skew: 0.00
22-pole: -0.05	22-skew: -0.01
24-pole: -0.01	24-skew: 0.01
26-pole: 0.01	26-skew: -0.00
28-pole: 0.00	28-skew: 0.00
30-pole: -0.00	30-skew: -0.00
32-pole: 0.00	32-skew: -0.00
34-pole: -0.00	34-skew: 0.00

Amplitudes in units: (norm=270.095)

2-pole: -115.86	2-skew: -74.80
4-pole: 10000.00	4-skew: 220.91
6-pole: 40.11	6-skew: -56.84
8-pole: -6.03	8-skew: -8.19
10-pole: -5.38	10-skew: -6.89
12-pole: 3.98	12-skew: 5.87
14-pole: -1.87	14-skew: 7.00
16-pole: -0.32	16-skew: 2.79
18-pole: -0.53	18-skew: 0.48
20-pole: 0.34	20-skew: -0.04
22-pole: -0.05	22-skew: -0.03
24-pole: -0.01	24-skew: -0.04
26-pole: -0.02	26-skew: -0.04
28-pole: 0.00	28-skew: -0.00
30-pole: -0.00	30-skew: 0.00
32-pole: 0.00	32-skew: -0.00
34-pole: -0.00	34-skew: -0.00

The two magnets QF and BD behave very similarly in terms of average field error size. The field errors also ought to scale linearly with the magnetisation error size. The real magnets ordered from Shin-Etsu Corporation in the previous section had total errors ranging from 26-67 units, with an average of 39, suggesting slightly (~33%) worse tolerances than the 1%/0.57° case.

6.3. Field Quality Improvement after Iron Wire Shimming

The pieces from eRHIC magnet #5 were re-used to make a magnet that lacked the dodecapole error and served as a test-bed for shimming, as shown in the figure below.

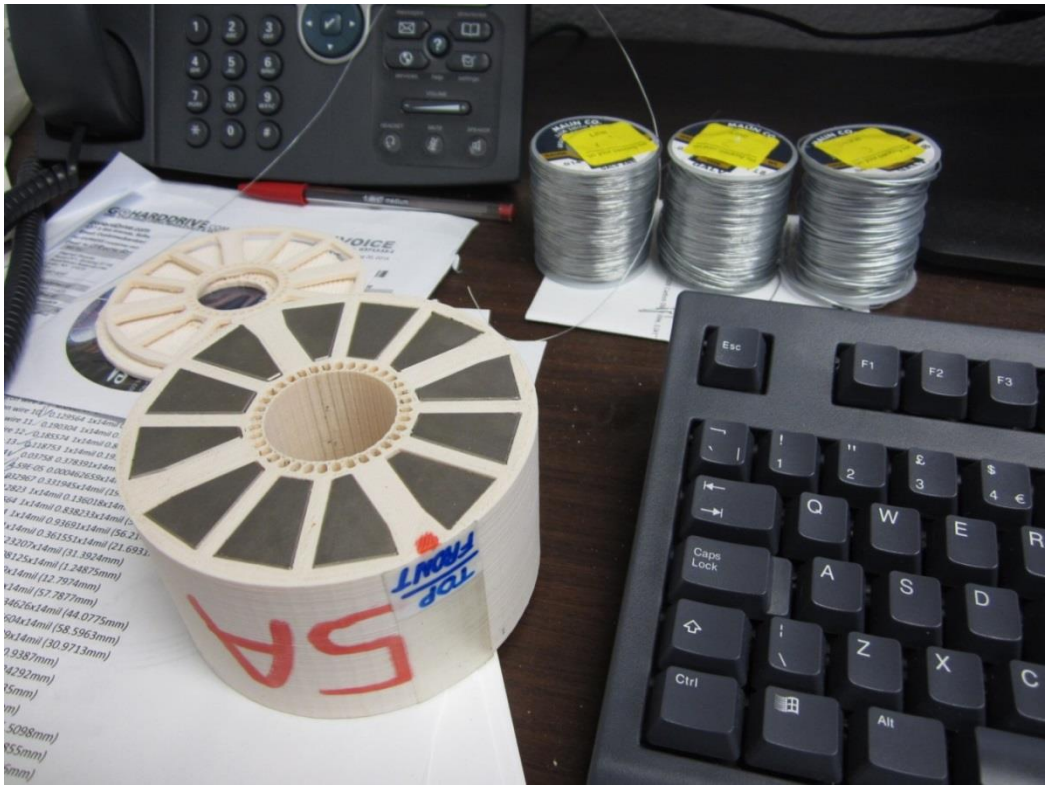

Figure. The pieces of the eRHIC LDRD Halbach magnet placed in a new 3D-printed holder to form magnet “5A”. This is a corrected Halbach quadrupole whose holder incorporates holes for iron shims to be placed around the inside of the bore (iron wire grades shown in background).

The shimming method is that of “floating” iron shims, operating on the principle that a narrow iron cylinder placed in an ambient magnetic field will be magnetised in the same direction as the field. Provided the field is not so high that the iron saturates (assuming mu=infinity for the iron), the magnetisation will be proportional to the ambient field magnitude. The shim field contribution from the uniformly transversely magnetised iron cylinder is the same as that of a cos(theta) superconducting dipole of the same dimensions: that is, an ideal external dipole field. The dipole moment is proportional to both the ambient field and the cross-sectional area of the shim.

An analytic field model of these iron wires was added to PM2D and 36 of the wires were placed at 10 degree intervals around the inner bore of the magnet. The code was asked to vary the radii (areas) of the wires in order to cancel the error multipoles observed in an initial measurement of the magnet with the rotating coil. The results of this process are shown in the table below.

Table. Rotating coil measurements of the shimming test magnet before shimming (Run 1_02), with sextupole-only correction (Run 2) and with all-multipole correction (Run 3) using iron wire shims.

eRHIC Permanent Magnet Quadrupoles PMQ_0005 & PMQ_005A (14-Oct-2015)

Field harmonics are in "units" of 10^{-4} of the quadrupole field at a reference radius of 10 mm.

Quantity	PMQ_0005 Run 2	PMQ_005A* Run 1_02(†)	PMQ_005A* Run 2(††)	PMQ_005A* Run 3(††)
Integrated Gradient (T)	1.9024	1.6501	1.6519	1.6537
Normal Dipole	--	--	--	--
Normal Quadrupole	10000.00	10000.00	10000.00	10000.00
Normal Sextupole	-11.95	**-19.46**	**-0.58**	0.87
Normal Octupole	3.61	5.61	5.21	3.12
Normal Decapole	3.86	-0.99	-0.84	-0.32
Normal Dodecapole	**-190.26**	**-1.03**	-1.06	0.55
Normal 14-pole	1.03	1.25	1.04	-0.03
Normal 16-pole	-1.31	-1.47	-1.52	-0.24
Normal 18-pole	0.07	0.12	0.13	0.05
Normal 20-pole	**-2.91**	**0.44**	0.40	-0.01
Normal 22-pole	-0.01	-0.03	-0.01	0.01
Normal 24-pole	0.04	0.05	0.03	-0.09
Normal 26-pole	-0.02	-0.01	-0.01	-0.03
Normal 28-pole	0.12	-0.12	-0.12	0.02
Normal 30-pole	0.00	0.00	0.00	0.00

Quantity	PMQ_0005 Run 2	PMQ_005A* Run 1_02(†)	PMQ_005A* Run 2(††)	PMQ_005A* Run 3(††)
Field Angle (mr)	--	--	--	--
Skew Dipole	--	--	--	--
Skew Quadrupole	--	--	--	--
Skew Sextupole	-5.28	**-6.42**	**-0.63**	-1.92
Skew Octupole	-18.51	-21.20	-21.18	**-1.45**
Skew Decapole	-8.52	-4.02	-4.23	**-0.70**
Skew Dodecapole	**-4.96**	**0.22**	0.32	-1.07
Skew 14-pole	0.85	0.07	-0.16	-0.51
Skew 16-pole	-0.13	-0.31	-0.33	-0.30
Skew 18-pole	0.10	-0.05	-0.06	-0.22
Skew 20-pole	0.01	0.24	0.23	0.00
Skew 22-pole	0.00	0.00	0.01	0.06
Skew 24-pole	0.01	-0.01	-0.02	-0.03
Skew 26-pole	0.01	0.00	0.01	0.00
Skew 28-pole	0.00	0.00	0.00	0.02
Skew 30-pole	0.00	0.00	0.00	0.00

* PMQ_005A is magnet built from magnets taken from PMQ_0005 and installed in a modified holder to reduce 12-pole

(†) *Magnet was measured with the magnet rotated 90 deg. about its axis, and flipped end-for-end, as compared to PMQ_005 measurements. The data were transformed in post-processing to correspond to the old orientation.*

(††) Runs 2 & 3 are measurement in PMQ_005A with two iterations of iron shims to reduce unallowed field harmonics.

(Note: Magnet name used for tesing was ERHIC-PMQ_0105 to avoid non-numeric serial number).

An initial shimming designed to cancel only the sextupole was highly successful, reducing the sextupole amplitude from 20.5 units to 0.86 units, while the rest of the multipoles stayed roughly the same. It should be noted there is some logic to the shim arrangement: for the sextupole shim (n=3) in a pure quadrupole background field (m=2), the shim pattern has pentagonal symmetry (n+m=5) and areas proportional to 1+cos(5 theta + phi) were used.

The optimiser was used to derive a shim distribution that would cancel all observed multipoles at once. The reduction was not as dramatic as with the sextupole alone, but reduced the quadrature sum of all error multipoles from 30.4 units to 4.34 units.

The rotating coil harmonics can be translated into polynomial fields with varying x across the y=0 midplane of the magnet, which is where the FFAG beam trajectories will be. These values are used in the figure below to calculate the relative error at any point across the aperture.

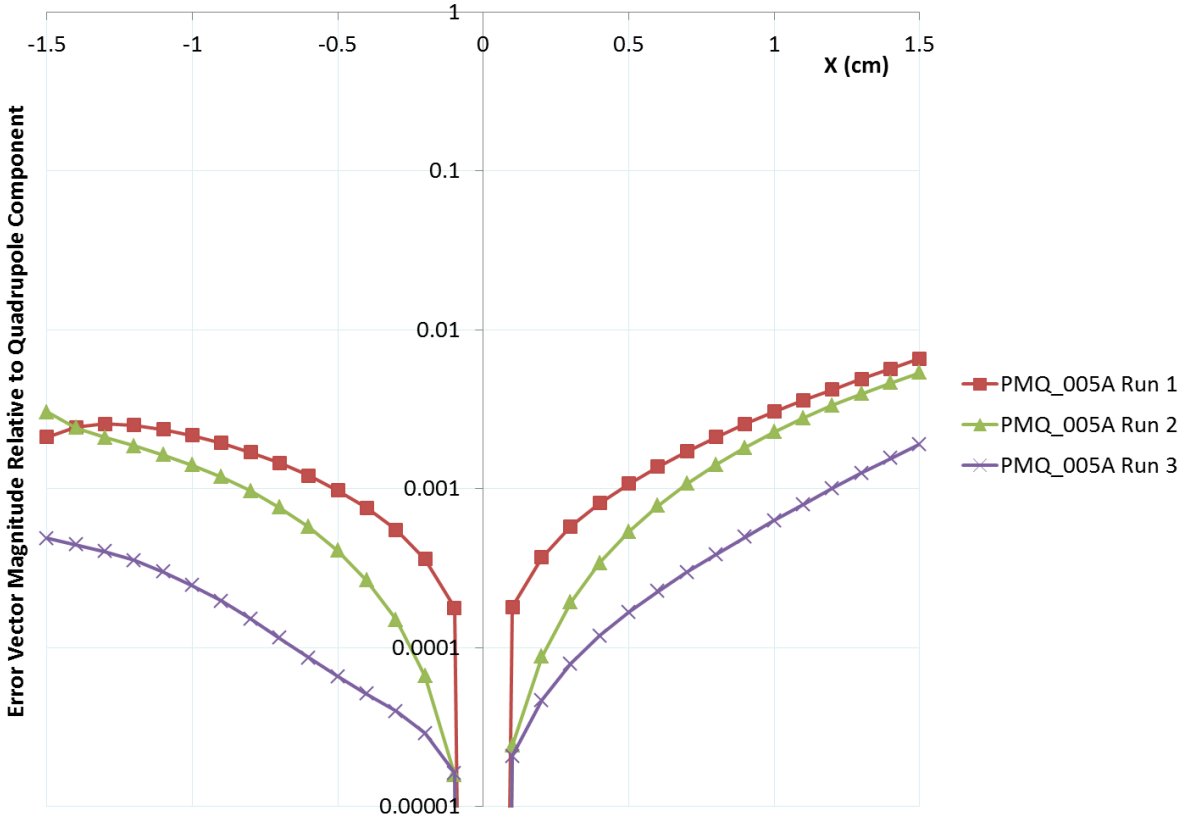

Figure. Relative field errors as a function of x on the y=0 midplane for the shimming test magnet: before shimming (Run 1, red); after sextupole cancellation (Run 2, green) and after all-multipole shimming (Run 3, purple).

Reading off the worst values at the “53% of magnet aperture” value relevant to Cbeta, this magnet had a 4.6e-3 relative field error on the midplane before shimming and a 1.2e-3 relative field error after shimming. This is almost good enough for the accelerator and shimming R&D continues to try and improve on this. Better models of saturation effects in the iron wires may help.

7. Plan for BNL Cbeta Halbach Prototypes

Purpose-built prototype magnets for Cbeta have also been ordered, including the "lopsided Halbach" magnet BD. Due to the 2-3 month magnet lead times, these are from an old lattice design Cell_Brooks_2015-12-11 rather than the most recent Cell_Smoothpipe_2016-02-04 presented in this report, but they are similar. Delivery of permanent magnet pieces should occur at the end of March 2016. A comparison of the magnets in the two versions is given in the table below.

Table. Comparison of current lattice Halbach magnets to those of the Cbeta prototypes ordered.

Parameter	QF current	QF prototype	BD current	BD prototype
Length	96.3mm	114.9mm	126.4mm	123.7mm
Gradient	-28.80 T/m	-23.62 T/m	19.19 T/m	19.12 T/m
Dipole at centre	0	0	-0.2680 T	-0.3768 T
Max good field radius	19.5mm	20.2mm	19.5mm	13.7mm
Min inner radius	36.5mm	37.2mm	36.5mm	30.7mm
Max outer radius	70.2mm	62.4mm	69.3mm	59.4mm
Max field in good field region	0.56 T	0.48 T	0.64 T	0.64 T
Max field at "pole tip"	1.05 T	0.88 T	0.97 T	0.96 T

These have been ordered from AllStar Magnetics rather than Shin-Etsu (due to cost reasons), which means a larger magnetisation angle error in the blocks of ±5 degrees as specified by their factory. Shimming methods will be tested to see if they can compensate for this larger error, possibly including shimming magnets instead of the iron wires.

8. Manufacturing Pipeline and Vendors

Discussions are starting with magnet manufacturing companies about what they can build for Cbeta. The pipeline of magnet manufacture and assembly onto the machine breaks down into the four stages below.

8.1. Permanent Magnet Wedges

These will be purchased, directly or indirectly, from a company. As mentioned previously, Shin-Etsu Corporation is a large manufacturer of the permanent magnet blocks with reasonably high quality. AllStar Magnetics has also provided BNL permanent magnets block in the past (for instance the radiation damage experiment), although they specify larger tolerances on their magnetisation angles. Electron Energy Corporation (EEC) has recently succeeded in an SBIR proposal for Cbeta and eRHIC magnet development worth ~$1M but this is spread over three years from April 2016 to April

2019. EEC manufactures both the blocks and magnet assemblies on-site in their machine shop. Finally, VacuumSchmelze GmbH has been contacted by Holger Witte for magnet blocks for the iron-poled quadrupole. Other companies not contacted yet include the undulator manufacturer KYMA.

Of these companies, AllStar generally provides the lowest cost but the least accurate magnetisation vector guarantee (±5 degrees). Shin-Etsu provides ±1 degree tolerance with some additional cost for tooling. EEC say even ±0.5 degrees is possible but there is an associated cost since additional steps of demagnetising the block, re-grinding it to an accurate shape and re-magnetising it have to occur.

8.2. Magnet Assembly

Although in theory this could be done on the BNL or Cornell sites, it seems that several companies are willing to bid for this work and are capable of doing it. EEC could be used as an end-to-end vendor for these first two steps. RadiaBeam LLC will make assemblies and girders but have to get the PM blocks from another company. They previously gave a cost estimate for assembling the Cbeta magnets and girders and are the only ones to have significant accelerator field experience (in fact they also make Halbach magnets for electron microscopes). Their absolute tolerances on positioning magnets on the girders were 0.1mm.

8.3. Shimming and Rotating Coil Measurements

Discussions so far with magnet manufacturers are indicating that the rotating coil is a specialised piece of measurement equipment for accelerator applications. None of the companies contacted so far have functioning rotating coils, although Radiabeam and EEC have Hall probes for field mapping. The shimming method works best using a rotating coil, so this stage is likely to be done in the BNL magnet division, where they have done it before.

8.4. Alignment and Girder

Since the magnets will need to be removed to do separate rotating coil and shimming steps, a fully integrated manufacture (measurement while on girder) does not look possible. Instead, survey fittings will be included in the non-magnetic body during the magnet assembly step and these will be used in the hall at Cornell to fit in with their on-site survey system. The survey references may also be used in the rotating coil stage to ensure alignment between the magnetic field and the magnet holder.

9. Early Cost Estimates for Wedge Blocks

For the whole FFAG part of the machine consisting of 148 FFAG cells (296 magnets), Shin-Etsu Corporation quoted a price of $725k for all the permanent magnet wedges, which included $24k of their own tooling to make the angles correct. Extrapolating AllStar Magnetics' price for 3 cells for the prototypes ($7698) to the full machine gives $380k, although bulk discounts may apply and this is with the looser tolerances on the magnetisation (5 degree angle rather than 1 degree).

The cost of the permanent magnet blocks does not dominate the cost of the FFAG, which includes magnet holders, correctors, girders etc. RadiaBeam LLC estimated a $1.45M cost for assembling holders for the wedges and aligning them onto girders. This excludes the wedges themselves and also does not include the correctors or their power supplies, which will be significant.